Supporting Online Material for

The Fern Sporangium: A Unique Catapult

X. Noblin,* N. O. Rojas, J. Westbrook, C. Llorens, M. Argentina, J. Dumais

*To whom correspondence should be addressed. E-mail: xavier.noblin@unice.fr

Published 16 March 2012, *Science* **335**, 1322 (2012)
DOI: 10.1126/science.1215985

This PDF file includes:

Other Supporting Online Material for this manuscript includes the following:
available at www.sciencemag.org/cgi/content/full/335/6074/1322/DC1

Materials and Methods

Sample preparation.

Sori were isolated from *Polypodium aureum* fronds. Sporangia were then separated from the sorus and stored in distilled water. At the beginning of an experiment, the sporangium pedicel was rapidly glued to a glass pipette in air and returned to water. The spores were then released by placing the sporangium in air. The process could be repeated many times by placing the empty sporangium in water for a few minutes, thus allowing the cavitation bubbles to dissolve.

Curvature measurements.

Sporangia were filmed from the side with a Phantom V7.3 or V7.11 high speed camera to observe the deformation of the annulus. Using custom-made image analysis tools in Matlab (The MathWorks inc., Natick, MA), we computed the deformation of the annulus, $\theta(s)$ (see Fig. S1 Left). We then deduced the mean curvature of the whole annulus: $\overline{K} = \left(\theta(S) - \theta(S=0)\right)/S$, S being the annulus length.

Force measurements.

We determined the bending rigidity EI of the annulus using a calibrated glass micropipette as a cantilever. We found: $EI \cong 1.0\ 10^{-10}\ N.m^2$.

SOM Text

Opening Model.

We describe in *[5]* the model that accounts for the change in annulus curvature during the slow (tens of seconds) opening phase. The opening dynamics is determined by three processes: the flux of water out of the cells (through a thin cellulosic cell wall acting as a semi-permeable membrane), the collapsing cell geometry, and the annulus elastic deformation. From the annulus stiffness, defined as: $B = 2EI/\left(lb^2\right) \cong 570\ N.m^{-1}$ (see Fig. S1 Left for cells geometry), we determined the negative pressure reached in the cells before cavitation.

Closing Model.

The fast closing of the annulus corresponds to the motion of a deformed beam that springs back. Due to various forces (inertial, elastic and dissipative) the motion presents different time scales. External friction is negligible, the dissipation is mainly internal and due to poroelasticity. The first inertial return phase accounts for 30-40 % of the motion in about ten microseconds. Then the slower poroelastic relaxation goes to 80-85% recovering of the initial deformation in a few hundreds of milliseconds. The last 15 % of the deformation are only recovered when the sporangium is dipped into pure water, the bubbles dissolve and the pressure recovers to a higher, positive value.

So the interesting stopping motion after the inertial phase happens after a 30-40% release of the initial curvature. Due to the presence of the bubble, the asymptotic curvature of the annulus is not the initial one.

The cavitation bubbles growth dynamics is so short compared to the initial closure of the annulus (by one or two order of magnitude) than it cannot account for the annulus dynamics observed. The characteristic speed for the cavitation bubble growth is given by a balance of the negative pressure difference $\Delta P = P_V - P$ with the inertial pressure ρU^2: $U = \sqrt{\Delta P / \rho}$. The tension before the cavitation event is of order 10 MPa, and we expect then to have *U*=100 m/s for the growth speed. Consequently, it takes less than one tenth of microsecond for the bubble to grow inside a cavity of tens of microns. This time scale is small compared to the observed time scale (25 microseconds), indicating that the dynamics of the bubble is slaved to the poroelastic dynamics. However, the cavitation dynamics is significant in one way – the cavitation of one cell sends a mechanical signal (pressure wave) that will cause neighboring cells to cavitate. Given that the bubble growth speed is about 100 m/s and the speed of sound in water exceeds 1000 m/s, this explains why several cells appear to cavitate instantaneously. Note that the cavitated cells are not always contiguous but can be separated by non-cavitated cells Fig. S2. Thus, it seems every cell must cavitate independently either by reaching first the critical tension or in response to the shock wave sent by the first cell to cavitate. Unfortunately, none of these events can be observed directly with current highspeed equipment.

The hypothesis of the internal dissipation for the second closing phase is confirmed by the similarity in the dynamics of sporangia in air and in water solution. We used a poroelastic beam model *[8]* to predict the complex dynamics of the closing phase. Here, we present a simpler version in terms of a spring mass system made of a viscoelastic medium derived directly from the poroelastic framework. The dynamics can be described by:

(Eq.S1) $$m\ddot{x} = -k_e x + \sum_{i=0}^{i=\infty} \sigma_i$$

(Eq.S2) $$\dot{\sigma}_i + \frac{1}{\tau_i}\sigma_i = k_i \dot{x}$$

m is the mass and x the deformation of the annulus, k_e is the stiffness of the main spring. The couples k_i, τ_i define pairs of springs/dashpots. The characteristic times are short enough to eliminate adiabatically the dynamics of the $\sigma_{i>1}$ since they rapidly tend to the value $k_i \tau_i \dot{x}$. We then get (see model on Fig. S2):

(Eq.S3) $$\ddot{x} + \frac{\dot{x}}{\tau} + \frac{k_e}{m} x = \sigma_0 + \sigma_1$$

(Eq.S4) $$\dot{\sigma}_{0,1} + \frac{1}{\tau_{0,1}}\sigma_{0,1} = k_{0,1}\dot{x}$$

Where $\frac{1}{\tau} = \sum_{i=2}^{i=\infty} \frac{k_i \tau_i}{m}$.

In our case, the time scales are well separated so that the solution of Eq.S3 and S4 corresponds to an inertial motion with oscillations (right term of Eq.S3 is constant), followed by exponential relaxations of the curvature with two larger time scales τ_1 and τ_0. The two first terms on the left side of Eq.S3 become negligible.

The curvature then varies as:

(Eq.S5) $K(t) = A\cos(\omega_0 t + \varphi)e^{-t/\tau} + Be^{-t/\tau_0} + Ce^{-t/\tau_1} + D$

The two relaxation times associated to the poroelastic dynamics are $\tau_0 \approx \frac{\eta c^2}{kE}$ and $\tau_1 \approx \beta\tau_0$ with β an integer of order 10 (we found a mean value around 14). We took η = 10^{-3} Pa.s, k=10^{-21} m^2 (which corresponds to a pore diameter d ~ 2 nm, close to values found in various species *[9]*, using: $k=\phi d^2/96$ and a porosity of 10 %), $c^* = 10\mu m$ the effective thickness of the beam, larger than c due to the annulus reinforcing structure and $E = 8GPa$, both being coherent with the force measurements giving EI. We then predict $\tau_0 \approx 3\,ms$. Both the opening and closing of the sporangium involve water flowing across a cellulosic cell wall. The different cellular faces of the annulus present walls that may differ slightly in composition and structure but to a first approximation we may expect them to have similar pore sizes and permeability (they belong to the same cell and the plasma membrane seems to be irrelevant here). The outer wall is indeed at least 1 µm thick as seen in Fig 57 of *[10]*. From our kinematic data on sporangium opening *[5]*, multiplying the cell conductivity by the membrane thickness and the water viscosity, we find an estimate for k of order 10^{-22} m^2, a little smaller than the value deduced from pore size.

$\omega_0 = \frac{2\pi}{T_0} \approx 3.52\sqrt{\frac{EI}{\rho' lbn^4 a^4}}$ is the natural pulsation of the beam inertial oscillations, by taking a=25µm, n=13, b=50µm, l=80µm, ρ'=500 kg.m^{-3} an effective density due to water evaporation, we then predict $T_0 \approx 27\mu s$.

Both time scales are in very good agreement with our measurements taken on 5 different movies and sporangium. Another curve taken from a high speed movie, showing clearly both oscillations and relaxation, is presented in Fig. S3.

We reproduce this closing dynamics using a macroscopic poroelastic beam made of a polymeric hydrogel with pore size similar to the cell wall of the annulus, i.e. a few nanometers in diameter. This experiment shows that the poroelastic characteristics of a beam (without the effects of bubbles dynamics) are sufficient to produce inertial oscillations followed by poroelastic relaxation, as seen in the movie S4. The temporal evolution of the beam tip fits very well with our Eq. S5. We believe this simple experiment reinforce our message that a poroelastic material such as the cellulosic cell wall can easily exhibit two time scales in its recoil dynamics.

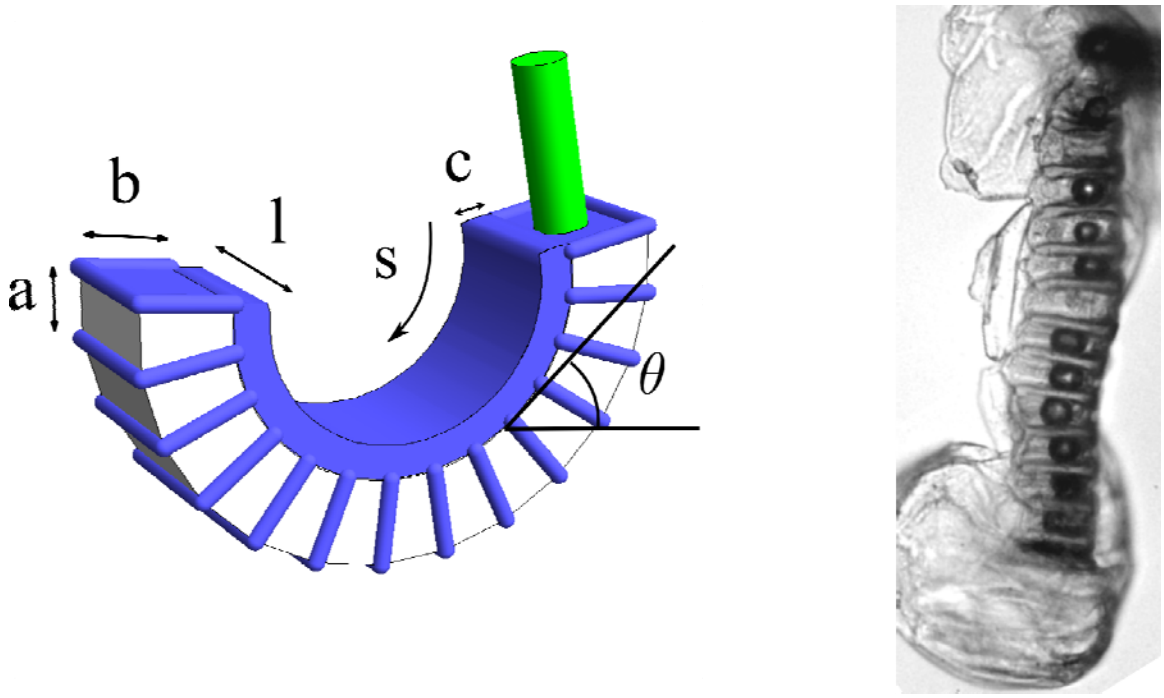

Fig. S1.
Left: Geometry of the sporangium. Right: dorsal view of a sporangium just after cavitation; note that a few cells have no bubble.

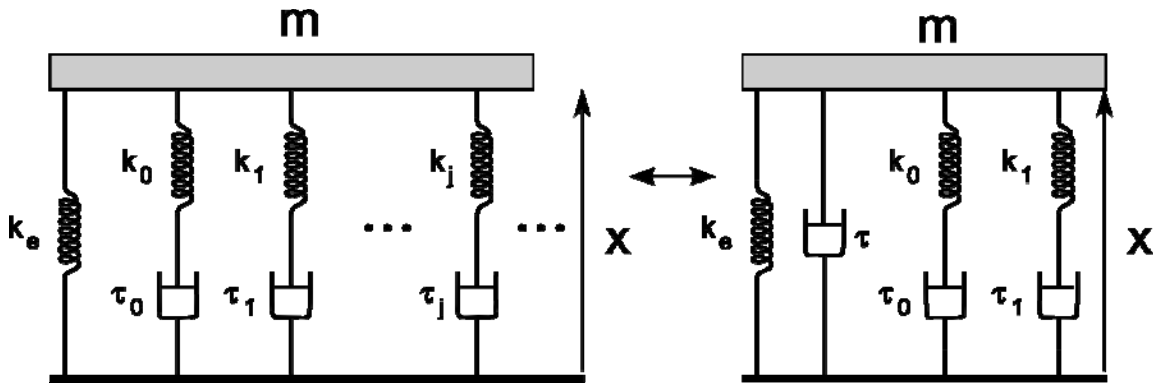

Fig. S2.

Mechanical representation of the annulus simplified by an adiabatic approximation for $i>1$.

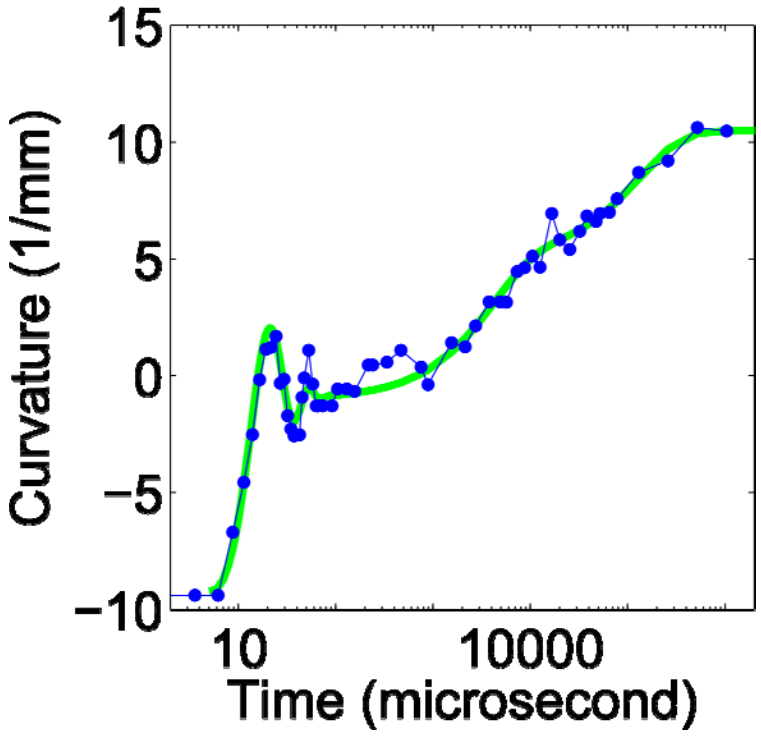

Fig. S3.

Another example of the fast closing dynamics with both inertial (with curvature oscillations) and poroelastic (exponential relaxation) time scales.

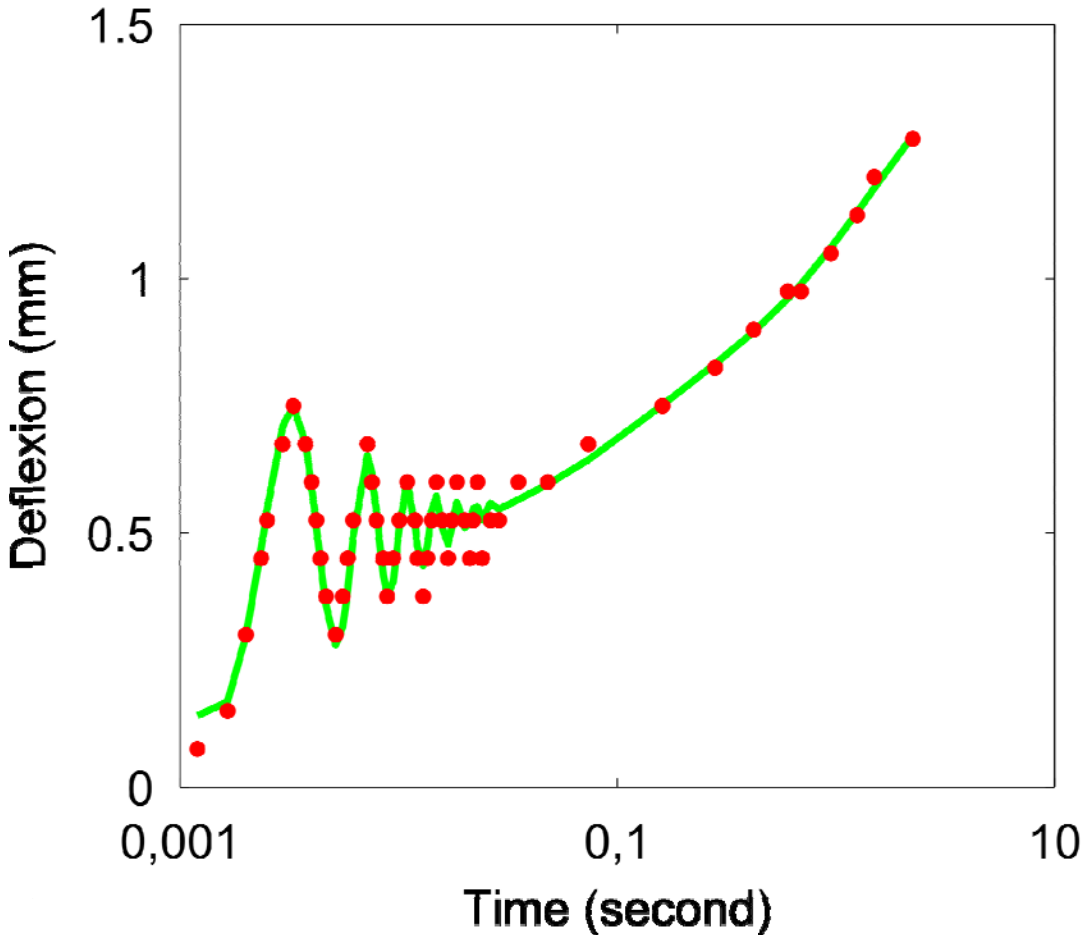

Fig. S4.
Beam deflexion vs. time for an artificial polymeric hydrogel beam from movie S4.

Movie S1

Slow opening motion (1215985MS1_opening.avi): 1 fps, playing at 5 fps.

Movie S2

Fast closing in air (1215985MS2_closing_air.avi): 125000 fps, playing at 12 fps. Inertial oscillations are clearly visible.

Movie S3

Fast closing in an osmotic solution (1215985MS3_closing_solution.avi): 80000 fps, playing at 100 fps.

Movie S4

Two time scales recoil of an artificial poroelastic polymeric beam (1215985MS4_poroelastic_beam.avi): 1000 fps, playing at 10 fps. Last 7 images separated by 0.25 s. Beam length: 20 mm.

References and Notes

1. C. T. Ingold, *Spore Liberation* (Clarendon, Oxford, 1965).

2. X. Noblin, S. Yang, J. Dumais, Surface tension propulsion of fungal spores. *J. Exp. Biol.* **212**, 2835 (2009). doi:10.1242/jeb.029975 Medline

3. O. Renner, *Jahrb. Wiss. Bot.* **56**, 647 (1915).

4. A. Ursprung, *Ber. Dtsch. Bot. Ges.* **33**, 153 (1915).

5. X. Noblin *et al*., in *Proceedings of the 6th Plant Biomechanics Conference*, Cayenne, French Guyana, 16 to 21 November 2009.

6. K. T. Ritman, J. A. Milburn, The acoustic detection of cavitation in fern sporangia. *J. Exp. Bot.* **41**, 1157 (1990). doi:10.1093/jxb/41.9.1157

7. A. L. King, The spore discharge mechanism of common ferns. *Proc. Natl. Acad. Sci. U.S.A.* **30**, 155 (1944). doi:10.1073/pnas.30.7.155 Medline

8. J. M. Skotheim, L. Mahadevan, Dynamics of poroelastic filaments. *Proc. R. Soc. Lond. A* **460**, 1995 (2004). doi:10.1098/rspa.2003.1270

9. N. Carpita, D. Sabularse, D. Montezinos, D. P. Delmer, Determination of the pore size of cell walls of living plant cells. *Science* **205**, 1144 (1979). doi:10.1126/science.205.4411.1144 Medline

10. K. Haider, Zur Morphologie und Physiologie der Sporangien leptosporangiater Farne. *Planta* **44**, 370 (1954). doi:10.1007/BF01940087